On negative streamers: A deterministic approach

Manuel Arrayás[a)]
Universidad Rey Juan Carlos, Dept. de Física, Tulipán s/n, 28933, Móstoles, Madrid, Spain

(Received 19 November 2003; accepted 21 May 2004)

The formation of streamers and spontaneous branching is commonly observed in dielectric breakdown phenomena. We discuss a deterministic streamer model that explains branching phenomena in terms of a Laplacian instability similar to that found in viscous fingering. Particular attention is paid to the physical interpretation of the model. © *2004 American Association of Physics Teachers.*

[DOI: 10.1119/1.1773175]

I. INTRODUCTION

If we apply an electric field to a volume filled with neutral particles, electric current will not flow through the volume, because there are no charged particles present. Thus, a volume filled with a gas of atoms is an almost ideal insulator. Air is a good example of such an insulator. A cubic centimeter of air contains roughly 2.7×10^{19} molecules of oxygen (O_2), nitrogen (N_2), water vapor, and some other gases. The charged particles are bound by powerful electric forces to form electrically neutral atoms and molecules, and as a result the air is an excellent insulator.

If a strong electric field is applied to matter of low conductivity and some electrons or ions are created, then the few mobile charges can generate an avalanche of more charges by impact ionization. A low temperature plasma is created, resulting in an electric discharge. Examples range from natural phenomena such as lightning and St. Elmo's fire[1] to neon tubes, TV displays,[2] and industrial plasma reactors for combustion gas cleaning.[3]

Discharges are nonequilibrium processes that occur in initially nonionized matter exposed to a strong electric field. Understanding the basic mechanisms of an electric discharge is a challenging problem involving ideas from nonequilibrium thermodynamics, atomic physics, electromagnetism, and pattern formation. Discharges can assume many different modes of appearance depending on the spatial and temporal characteristics of the electric field and on the ionization and charge transport properties of the medium. Phenomenologically, discharges can be classified into stationary ones, such as arc, glow or dark discharges, and transient ones, such as sparks and leaders.[4] The distinction between the various discharge phenomena varies among authors.

A streamer is a sharp ionization wave that propagates into a nonionized gas, leaving a nonequilibrium plasma behind. They have been reported in early stages of atmospheric discharges[5] such as sparks or sprite discharges.[6] Streamers can split into branches spontaneously, but how this branching is precisely determined by the underlying physics is an open question.

To model the initial stage of dielectric breakdown, when a gas suddenly changes from being an insulating dielectric to a conducting gas, Raether[7] characterized rare long-range photo-ionization events as stochastic processes that enhance ionization avalanches. The idea is that photons, which have been created by atoms that previous collisions have excited, initiate secondary avalanches. In this scenario, avalanches are randomly distributed at differents points near the streamer head. Some phenomenological stochastic models for dielectric breakdown have been proposed[8] since then. Branching would occur due to randomly distributed ionization avalanches.

We use a fully deterministic fluid model with pure impact ionization. It was a surprise that anode directed streamers become unstable and develop branching. We have proposed a branching mechanism that is qualitatively different from other mechanisms.[9] This mechanism for branching is related to a Laplacian interfacial instability. There are other systems such as solidification or viscous fingers in which the normal growth velocity is proportional to the gradient of a bulk field which obeys a Laplace or diffusion type of equations. For the reader interested in these examples of instabilities and their comparison to with streamer calculations presented here, we suggest Ref. 10.

If the gas density is low, it could be argued that the fluid model is no longer valid and a statistical description in terms of molecular dynamics or kinetic theory would be more suitable. How individual processes at the atomic scale are related to the macroscopic or mesoscopic physics is a fundamental question without an easy answer. This question needs to be answered if the branching mechanism discussed here is to be modeled using stochastic dielectric breakdown simulations.

In this paper we will introduce the fluid model that incorporates the physical ingredients needed to describe a nonattaching[11] gas such as nitrogen under normal conditions. In Sec. III some numerical simulations based on this model are discussed. In Sec. IV streamer branching is investigated analytically and the main results for stationary planar fronts are summarized. In Sec. V we discuss our results for shock fronts, and in Sec. VI we study the stability of the planar shock front. In Sec. VII we obtain the asymptotic behavior of the dispersion relation, and in Sec. VIII we finish with a summary and discussion of future work that is needed.

II. THE STREAMER MODEL

In this section we present a *minimal streamer model*, that is, a fluid approximation with local field-dependent impact ionization reactions in a nonattaching gas like argon or nitrogen.[12]

The balance equations for electrons and ions are

$$\partial_\tau n_e + \nabla_{\mathbf{R}}\cdot\mathbf{j}_e = S \tag{1a}$$

$$\partial_\tau n_i + \nabla_{\mathbf{R}}\cdot\mathbf{j}_i = S, \tag{1b}$$

where $n_{e,i}$ and $\mathbf{j}_{e,i}$ are the particle densities and currents of electrons and ions, respectively, and S is the source term. The fact that the source terms on the right-hand side of Eqs.

(1a) and (1b) are equal is due to conservation of charge in an ionization event.

The electron particle current $\mathbf{j}_e$ is approximated as the sum of a drift and diffusion term

$$\mathbf{j}_e = -\mu_e \mathcal{E} n_e - D_e \nabla_{\mathbf{R}} n_e, \tag{2}$$

where $\mathcal{E}$ is the electric field and μ_e and D_e are the mobility and diffusion coefficient of the electrons. In equilibrium, the kinetic theory of gases links diffusion to mobility through the Einstein relation $D_e/\mu_e = kT/e$. For anode-directed streamers, the ion current can be neglected because it is more than two orders of magnitude smaller than the electron one, so we will take

$$\mathbf{j}_i = 0. \tag{3}$$

The electric field due to the charged particles is determined by Poisson's equation

$$\nabla_{\mathbf{R}} \cdot \mathcal{E} = e(n_i - n_e)/\varepsilon_0. \tag{4}$$

The coupling between the space charges and the electric field makes the problem nonlinear.

The source term S accounts for the creation of free charges by impact ionization. Initially, an electron liberated by an outside agent, such as radiation, is accelerated in a strong local field. The electron collides with a neutral molecule and ionizes it. The result is generation of new free electrons and a positive ion. This ionization rate is given by the product of the drift current of free electrons $|\mu_e \mathcal{E} n_e|$ and the ionization coefficient $\alpha(|\mathcal{E}|)$. The ionization coefficient is related to the density of the neutral particles of the gas and their effective ionization cross sections and represents the inverse of the ionization mean free path. The calculation from first principles of this coefficient is not easy. Townsend gave a phenomenological approximation[4] by treating it as a process activated by drift energy gained from the field $e\lambda|\mathcal{E}|$ (λ is the total scattering mean free path), with activation energy Δ. These considerations lead to a formula analogous to that of Arrhenius for thermally activated processes

$$\alpha(|\mathcal{E}|) = \frac{C}{\lambda} \exp\left(\frac{-\Delta}{e\lambda|\mathcal{E}|}\right) = \alpha_0 \exp\left(\frac{-\mathcal{E}_0}{|\mathcal{E}|}\right), \tag{5}$$

where C is a dimensionless constant and $\mathcal{E}_0 = \Delta/e\lambda$ has dimensions of electric field. So the source term is

$$S = |\mu_e \mathcal{E} n_e| \alpha_0 \exp(-\mathcal{E}_0/|\mathcal{E}|). \tag{6}$$

In the source term (6), the ionization due to the photons created by recombination or scattering events is neglected. This neglect is justified if the cross section of the photoionization process is much smaller than that due to electrons. Photoionization can be taken into account, but the dynamical equations would become nonlocal. In attaching gases like oxygen, a third kind of charged species needs to be taken into account, namely, negative ions formed by a neutral molecule catching a free electron.[13]

Note that our balance equations, (1a) and (1b), are deterministic, and stochastic effects are not included in the model.

We need to specify the appropriate boundary and initial conditions. We ignore the details of the plasma initiation event (for example, triggering by radiation from an external source), and assume that at $t=0$ a small well-localized ionization seed is present. We make this assumption clearer in the following. Boundary conditions will be discussed in Sec. III.

To identify the physical scales and the intrinsic parameters of the model, it is convenient to reduce the equations to dimensionless form. The natural units are given by the ionization length $R_0 = \alpha_0^{-1}$, the characteristic impact ionization field $\mathcal{E}_0$, and the electron mobility μ_e, which leads to the velocity scale $v_0 = \mu_e \mathcal{E}_0$, and the time scale $\tau_0 = R_0/v_0$. The values for these quantities for nitrogen at normal conditions are $\alpha_0^{-1} \approx 2.3$ μm, $\mathcal{E}_0 \approx 200$ kV/m, and $\mu_e \approx 380$ cm^2/V s. We introduce the dimensionless variables[12] $\mathbf{r} = \mathbf{R}/R_0$, $t = \tau/\tau_0$, the dimensionless field $\mathbf{E} = \mathcal{E}/\mathcal{E}_0$, the dimensionless electron and ion particle densities $\sigma = n_e/n_0$ and $\rho = n_i/n_0$ with $n_0 = \varepsilon_0 \mathcal{E}_0/(eR_0)$, and the dimensionless diffusion constant $D = D_e/(R_0 v_0)$.

In terms of dimensionless variables, the model equations become

$$\partial_t \rho_e - \nabla \cdot \mathbf{j} = \rho_e f(|\mathbf{E}|), \tag{7}$$

$$\partial_t \rho_i = \rho_e f(|\mathbf{E}|), \tag{8}$$

$$\rho_i - \rho_e = \nabla \cdot \mathbf{E}, \tag{9}$$

$$\rho_e \mathbf{E} + D \nabla \rho_e = \mathbf{j}. \tag{10}$$

The function $f(|\mathbf{E}|)$ from Townsend's approximation is

$$f(|\mathbf{E}|) = |\mathbf{E}| \alpha(|\mathbf{E}|) = |\mathbf{E}| \exp(-1/|\mathbf{E}|). \tag{11}$$

III. SIMULATIONS

In confined geometries streamers usually have a nontrivial finger-like shape. In general, two regions can be observed. The interior of the streamer is an ionized region that is quasineutral and equipotential. The outer region is filled with the nonionized gas. These two regions are separated by a very narrow region in which most of the ionization process is taking place. In this same space there is a nonzero charge density and consequently a very large electric field gradient. This is one of the reasons why accurate simulations are rather demanding. These features are strongly reminiscent of what occurs in combustion fronts[14] and viscous fingering.[15]

We discuss the numerical simulations of the streamer model based on Eqs. (7)–(11). We assume cylindrical symmetry. A planar cathode is located at $z=0$ and a planar anode is at $z=2000$. The radial coordinate extends from the origin up to $r=2000$ to avoid lateral boundary effects on the field configuration. The stationary potential difference between the electrodes, $\Delta\Phi = 1000$, corresponds to a uniform background field $\mathbf{E} = -0.5\,\mathbf{e}_z$, where $\mathbf{e}_z$ is the unit vector in the z direction. For nitrogen under normal conditions, the separation of the electrodes corresponds to 5 mm and a potential difference of 50 kV. We choose $D = 0.1$, which is appropriate for nitrogen, and as the initial condition an electrically neutral Gaussian ionization seed on the cathode

$$\rho_e(r, z = , t = 0) = \rho_i(r, z, t = 0) = 10^{-6} e^{-(z^2 + r^2)/100^2}. \tag{12}$$

At the electrodes we take no flux of charges as boundary conditions, so we use homogeneous Neumann conditions for the charge densities.

The parameters of the simulation are essentially the same as in the earlier simulations of Ref. 16 except that our background electric field is twice as large; the earlier work had 25

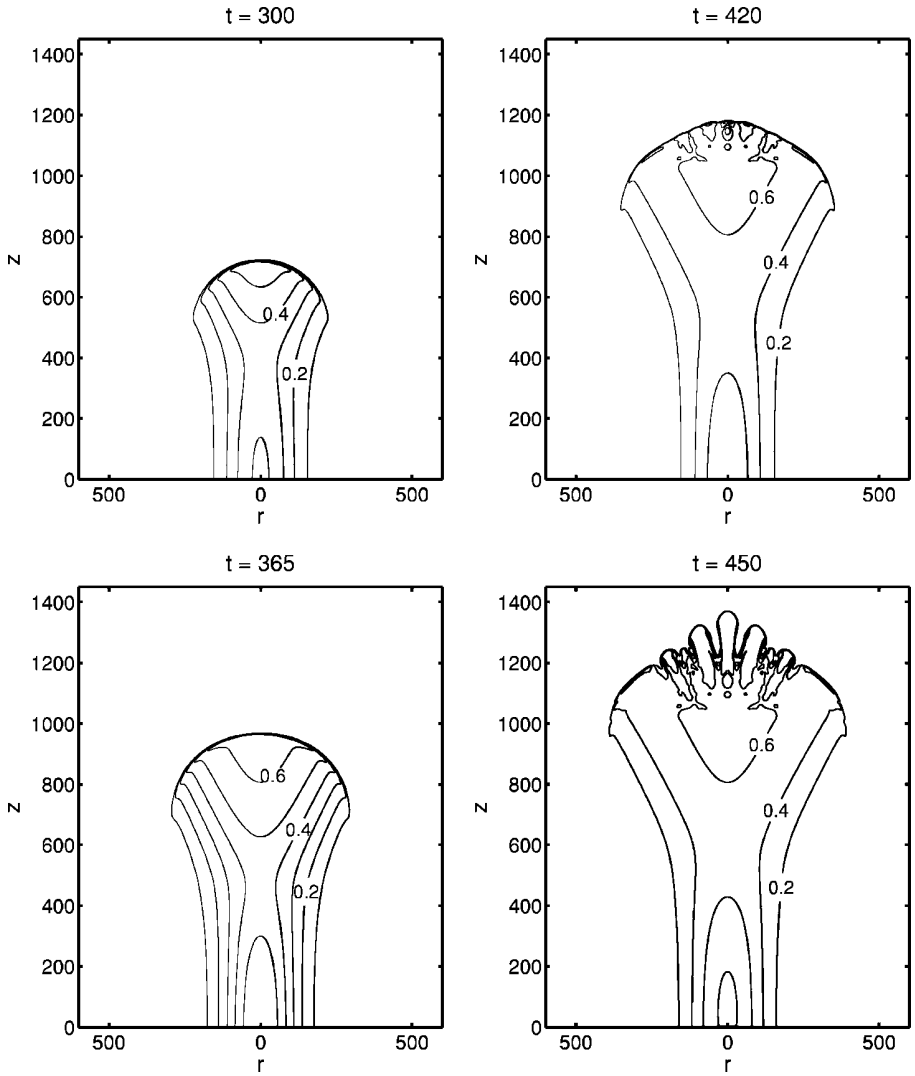

Fig. 1. Evolution of spontaneous branching of anode directed streamers in a strong homogeneous background field at times $t=300$, 365, 420, and 450. The model and initial and boundary conditions are discussed in the text. The planar cathode is located at $z=0$ and the planar anode is at $z=2000$ (shown is $0 \leqslant z \leqslant 1400$). The radial coordinate extends from the origin up to $r=2000$ (shown is $0 \leqslant r \leqslant 600$). The lines denote levels of equal electron density ρ_e with increments of 0.2 as indicated by the labels.

kV applied over a gap of 5 mm. These parameters correspond to a dimensionless background field of 0.25, and branching was not observed.

We used uniform space–time grids with a spatial mesh of 1000×1000. The spatial discretization is based on local mass balances. The diffusive fluxes are approximated in standard fashion with second-order accuracy. For the convective fluxes a third-order upwind-biased formula was chosen to reduce the numerical oscillations that are common with second-order central fluxes. Such oscillations can be completely avoided, for example, by flux-limiting, but preliminary tests showed that the upwind-biased formula already gives sufficient numerical monotonicity and is much faster. Time stepping is based on an explicit linear two-step method, where at each time step the Poisson equation is solved by the FISHPACK routine. References for these procedures can be found in Ref. 17.

In Fig. 1 we can see the results of some of the simulations of the model. The evolution of a negative streamer toward the anode is displayed, and the development of branching[7] is observed. Such branching phenomena have been observed in some simulations with improved accuracy and different boundary and initial conditions.[18] There have been some discussions of the possibility of this branching being a numerical artifact.[19] In the following sections we will see some analytical evidence that this branching is due to an intrinsic instability of the equations of the model.

IV. THE ONE-DIMENSIONAL STREAMER EQUATIONS IN A COMOVING FRAME: THE PLANAR FRONT

In Sec. III some numerical evidence of branching was presented. We now investigate the existence of branching by analytical methods. We will start with the solution for a stationary planar front. The idea is to find a uniformly translating front and investigate how the transverse perturbation of this solution will develop.

For planar fronts, we assume that charge varies only in the z direction. Thus, Eqs. (7)–(10) become

$$\partial_t \rho_e - \partial_z(\rho_e E) - D\partial_z^2 \rho_e - \rho_e f(|E|) = 0, \tag{13a}$$

$$\partial_t \rho_i - \rho_e f(|E|) = 0, \tag{13b}$$

$$\partial_z E - \rho_i + \rho_e = 0. \tag{13c}$$

We will change our reference frame to a frame moving with velocity v in the z direction $(x,y,\xi=z-vt)$. Equation (13) becomes

$$\partial_t \rho_e = v\,\partial_\xi \rho_e + \partial_\xi(\rho_e E) + D\partial_\xi^2 \rho_e + \rho_e f(|E|), \tag{14a}$$

$$\partial_t \rho_i = v\,\partial_\xi \rho_i + \rho_e f(|E|), \tag{14b}$$

$$\partial_\xi E - \rho_i + \rho_e = 0. \tag{14c}$$

A front moving uniformly with velocity v in the fixed frame is stationary in this comoving frame, $\partial_t \rho_e = \partial_t \rho_i = 0$. As a result, the corresponding front profiles are solutions of ordinary differential equations.

We need to determine the boundary conditions. The field is completely screened in the ionized region and is approximately constant in space and time far ahead of the front. Hence, we take $\mathbf{E}$ as

$$\mathbf{E} = \begin{cases} 0 & (z \to -\infty), \\ E_\infty \mathbf{e}_z & (z \to +\infty), \end{cases} \tag{15}$$

where E_∞ is a constant. These boundary conditions imply that a time independent amount of charge is traveling within the front, and no currents flow far behind the front in the ionized regime.

For a nonvanishing far field E_∞, there is a continuous family of uniformly moving front solutions,[12,20] because the front propagates into an unstable state.[21] In particular, for $E_\infty > 0$ there is a solution for any velocity $v \geqslant 0$, and for $E_\infty < 0$, there is a solution for any $v \geqslant |E_\infty|$. These solutions are associated with an electron density profile that decays asymptotically for large ξ as $\rho_e(\xi) \propto e^{-\lambda \xi}$ with $\lambda \geqslant 0$. We refer the interested reader to Ref. 21.

In practice, not all these uniformly propagating solutions are observed, but only a specific one that it is called the selected front.[12,21] If initially the electron density strictly vanishes beyond a certain point ξ_0 (corresponding to $\lambda = \infty$), so that

$$\rho_e = 0 = \rho_i \quad \text{for } \xi > \xi_0 \quad \text{at } t = 0, \tag{16}$$

then the electron density will vanish for all times $t > 0$ in a coordinate system moving with velocity $v = |E_\infty|$, and an ionization front propagating with the electron drift velocity $|E_\infty|$ develops. In the remainder of the paper, we will consider this case.

In Fig. 2 we show the solution of Eq. (14) with the boundary conditions, Eqs. (15) and (16). We have chosen the far field $E_\infty = -1$ and the diffusion coefficient $D = 0.1$. The numerical calculations were done using a shooting method for solving our two-point boundary value problem.[22] This technique consists in choosing values for all of the dependent variables at one boundary. We then integrate the ordinary differential equations by initial value methods, arriving at the other boundary. In general, we find discrepancies with the desired boundary values there. Next we adjust the free parameters at the starting point to reduce the discrepancies at the other boundary. The idea is to iterate this procedure until we obtain the desired accuracy.

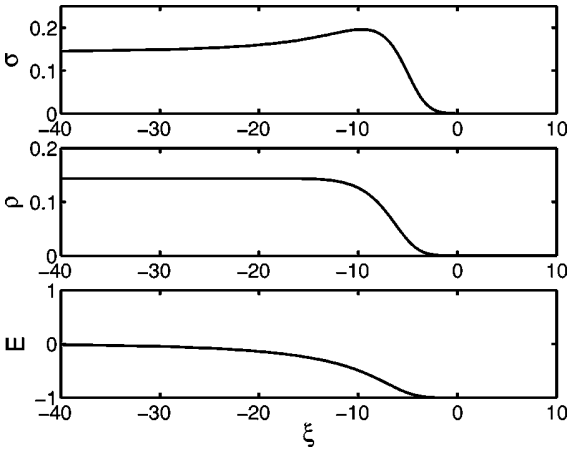

Fig. 2. Electron density ρ_e, ion density ρ_i, and electric field E for a negative ionization front moving with $v = |E_\infty|$ in the comoving frame. The far field is $E_\infty = -1$ and $D = 0.1$.

V. SHOCK FRONTS

We will simplify our model a bit more by taking the limit $D = 0$ in the streamer equations. It reduces the order of the equations and makes it possible to integrate them explicitly. Then, in the comoving frame, using Eq. (14), we have for a stationary front

$$v\,\partial_\xi \rho_e + \partial_\xi(\rho_e E) + \rho_e f(|E|) = 0, \tag{17}$$

$$v\,\partial_\xi \rho_i + \rho_e f(|E|) = 0, \tag{18}$$

$$\partial_\xi E - \rho_i + \rho_e = 0. \tag{19}$$

We can solve this system of equations analytically. If we subtract Eq. (18) from Eq. (17) and use Eq. (19) to eliminate $\rho_e - \rho_i$, we obtain

$$-v\,\partial_\xi E + \rho_e E = 0. \tag{20}$$

Equation (20) is a consequence of charge conservation as we can see by writing $\partial_t q + \nabla \cdot \mathbf{j}_{\text{tot}} = 0$, with the total charge defined as $q = \rho_i - \rho_e$. In our model each ionizing collision produces the same number of negative and positive charges, so we have $\nabla \cdot \mathbf{j}_{\text{tot}} = 0$. The total current is given by $\mathbf{j}_{\text{tot}} = \partial_t \mathbf{E} + \rho_e \mathbf{E}$, and for a planar front with constant and time independent field $\mathbf{E} = E_\infty \mathbf{e}_z$ in the nonionized region where $\rho_e = 0$, the total current $\mathbf{j}_{\text{tot}} = j_{\text{tot}}(t)\mathbf{e}_z$ vanishes. In the comoving frame of Eqs. (14) and (17)–(19), we arrive at Eq. (20).

The front equations reduce to two ordinary differential equations for ρ_e and E,

$$\partial_\xi[(v+E)\rho_e] = -\rho_e f(E), \quad f(E) = |E|\,\alpha(E), \tag{21}$$

$$v\,\partial_\xi \ln|E| = \rho_e, \tag{22}$$

which can be solved analytically to give

$$\rho_e[E] = \frac{v}{v+E}\,\rho_i[E], \tag{23}$$

$$\rho_i[E] = \int_{|E|}^{|E_\infty|} \frac{f(x)}{x}\,dx = \int_{|E|}^{|E_\infty|} \alpha(x)\,dx, \tag{24}$$

$$\xi_2 - \xi_1 = \int_{E(\xi_1)}^{E(\xi_2)} \frac{v+x}{\rho_i[x]}\,\frac{dx}{x}. \tag{25}$$

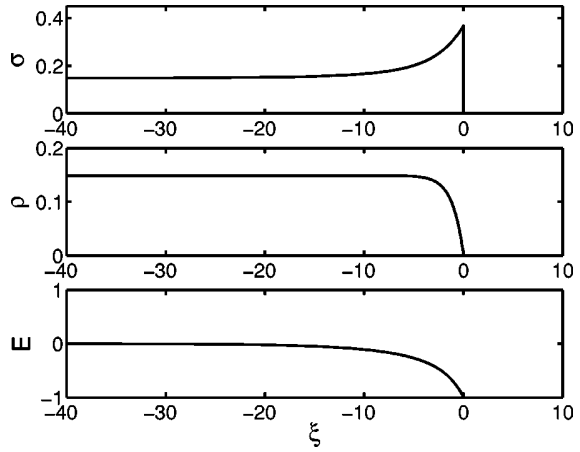

Fig. 3. The electron density ρ_e, ion density ρ_i, and electric field E for a negative ionization shock front moving with $v=|E_\infty|$ in the comoving frame. The far field is $E_\infty=-1$.

Equations (23) and (24) give ρ_e and ρ_i as a function of E, and the spatial dependence $E=E(\xi)$ is obtained implicitly, as $\xi=\xi(E)$ in Eq. (25). In Fig. 3 the solutions (23)–(25) for a shock front moving with $v=1$ are shown. We have chosen $\xi_1=0$ and $E(\xi_1)=E_\infty$.

VI. STUDY OF INSTABILITIES: CORRUGATION OF THE FRONT

The planar shock front may be unstable with respect to periodic perturbations on the surface of discontinuity which then form ''ripples'' or ''corrugations'' on the surface. In this case, we are interested in obtaining the dispersion relation to find which mode will grow faster and eventually determine the characteristic shape of the streamer. Here we will derive the perturbed equations and the boundary conditions.

Let the planar shock front that propagates into the z direction receive a small perturbation with an arbitrary dependence on the transverse coordinates x and y. Within linear perturbation theory, the perturbation can be decomposed into Fourier modes. Therefore we need the growth rate $s(k)$ of an arbitrary transverse Fourier mode to predict the evolution of an arbitrary perturbation. Because of isotropy within the (x,y) plane, we can restrict the analysis to Fourier modes in the x direction, and we consider linear perturbations $\propto\exp(st+ikx)$. This notation anticipates the exponential growth of such modes. A perturbation also will lead to a perturbation of the position of the ionization shock front. Hence, we introduce the variable $\zeta=\xi-\epsilon\exp(ikx+st)$ and the ansatz

$$\rho_e(x,\zeta,t)=\rho_{e0}(\zeta)+\epsilon\rho_{e1}(\zeta)e^{ikx+st}, \tag{26a}$$

$$\rho_i(x,\zeta,t)=\rho_{i0}(\zeta)+\epsilon\rho_{i1}(\zeta)e^{ikx+st}, \tag{26b}$$

$$\phi(x,\zeta,t)=\phi_0(\zeta)+\epsilon\phi_1(\zeta)e^{ikx+st}, \tag{26c}$$

where ρ_{e0}, ρ_{i0}, and ϕ_0 are the electron density, ion density, and electric potential of the planar ionization shock front obtained in Sec. V. Note, however, that these planar solutions are shifted to the position of the perturbed front. The substitution of Eq. (26) into Eq. (14) (with $D=0$) gives to leading order in the small parameter ϵ:

$$(v+E_0)\partial_\zeta\rho_{e1}=(s+2\rho_{e0}-\rho_{i0}-f)\rho_{e1}-\rho_{e0}\rho_{i1}+(\partial_\zeta\rho_{e0}-\rho_{e0}f')\partial_\zeta\phi_1-s\partial_\zeta\rho_{e0}, \tag{27a}$$

$$v\partial_\zeta\rho_{i1}=-f\rho_{e1}+s\rho_{i1}-\rho_{e0}f'\partial_\zeta\phi_1-s\partial_\zeta\rho_{i0}, \tag{27b}$$

$$(\partial_\zeta^2-k^2)\phi_1=\rho_{e1}-\rho_{i1}+k^2E_0. \tag{27c}$$

In Eq. (27) we denote $f=f(E_0)$, $f'=\partial_{|E|}f(|E|)|_{E_0}$, and $E_0=-\partial_\zeta\phi_0(\zeta)$ as the electric field of the uniformly translating front. In Eq. (27c), the term $k^2\phi_1$ arises as a consequence of the dependence of the electric potential on x. Equation (27) can be written in matrix form as

$$\partial_\zeta\begin{pmatrix}\rho_{e1}\\ \rho_{i1}\\ \psi_1\\ \phi_1\end{pmatrix}=\mathbf{M}_{s,k}\cdot\begin{pmatrix}\rho_{e1}\\ \rho_{i1}\\ \psi_1\\ \phi_1\end{pmatrix}-\begin{pmatrix}s\partial_\zeta\rho_{e0}/(v+E)\\ s\partial_\zeta\rho_{i0}/v\\ -Ek^2\\ 0\end{pmatrix}, \tag{28}$$

where

$$\mathbf{M}_{s,k}=\begin{pmatrix}\dfrac{s+2\rho_{e0}-f-\rho_{i0}}{v+E} & \dfrac{-\rho_{e0}}{v+E} & \dfrac{\partial_\zeta\rho_{e0}-\rho_{e0}f'}{v+E} & 0\\ \dfrac{-f}{v} & \dfrac{s}{v} & \dfrac{-\rho_{e0}f'}{v} & 0\\ 1 & -1 & 0 & k^2\\ 0 & 0 & 1 & 0\end{pmatrix}. \tag{29}$$

Note we have introduced an auxiliary field $\psi_1=\partial_\zeta\phi_1$, which is the positive derivative of the electric field to order ϵ.

Now that we have obtained the first-order perturbation equations, we can discuss the boundary conditions. First we consider the boundary conditions at $\zeta=0$. There are two types of boundary conditions, one arising from the boundedness of densities to the left of the shock front at $\zeta\to0^-$, and the other arising from the continuity of fields across the position $\zeta=0$ of the shock front. From Eq. (17) we find that $(v+E)\partial_z\rho_e$ is finite for all z, also for $z\to0^-$ and for $z=0$, because $(v+E)\partial_z\rho_e=\rho_e(\rho_e-\rho_i-f)$ is finite. The same is true for ρ_{e0}. In particular, $\int_{-l}^{l}dz(v+E)\partial_z\rho_{e0}\to0$ as $l\to0$, and $(v+E)\partial_z\rho_{e0}\to0$ as $z\to0^-$. Therefore we impose the same conditions for ρ_{e1}, namely

$$\lim_{l\to0}\int_{-l}^{l}d\zeta(v+E)\partial_\zeta\rho_{e1}=0, \tag{30}$$

$$\lim_{\zeta\to0^-}(v+E)\partial_\zeta\rho_{e1}=0. \tag{31}$$

We will now make use of the continuity conditions. We match the $\zeta<0$ solution to the $\zeta>0$ solution. In front of the shock there are no sources, and thus we have to solve $\nabla^2\phi=0$ for $\zeta>0$ and $\nabla\phi=-E_\infty\hat{z}=v\hat{z}$ when $\zeta\to\infty$. The solution to first order in ϵ has the form

$$\rho_e=0, \tag{32}$$

$$\rho_i=0 \quad \text{for } \zeta>0, \tag{33}$$

$$\phi=a+v\zeta+\epsilon(v+be^{-k\zeta})e^{ikx+st}, \tag{34}$$

with the undetermined integration constants a and b.

Now ρ_i and $\nabla\phi$ have to be continuous across the shock front; $\nabla\phi$ is continuous because the charge density $\rho_i-\rho_e$ is

finite everywhere. From Eq. (18) ρ_i is continuous, and ρ_e and $|\mathbf{E}|$ are bounded for all z. From the continuity of ρ_i, we have

$$\lim_{\zeta\to 0}[\rho_i(x,\zeta^+,t)-\rho_i(x,\zeta^-,t)]=0, \tag{35}$$

which implies that

$$\rho_{i1}(0)=0, \tag{36}$$

where we have used Eqs. (32) and (26) for the right and left limits.

The continuity of the electric field to first order in ϵ implies that

$$\lim_{\zeta\to 0}[\partial_\zeta\phi(x,\zeta,t)|_{\zeta^+}-\partial_\zeta\phi(x,\zeta,t)|_{\zeta^-}]=0, \tag{37a}$$

$$\lim_{\zeta\to 0}[\partial_x\phi(x,\zeta,t)|_{\zeta^+}-\partial_x\phi(x,\zeta,t)|_{\zeta^-}]=0. \tag{37b}$$

If we use Eqs. (32) and (26) again, these conditions become

$$\psi_1(0)=-kb, \quad \phi_1(0)=v+b. \tag{38}$$

If we impose the continuity of the potential, we obtain $a=\phi_0(0)$ and $\phi_1(0)=v+b$ (which is the same condition obtained from the continuity of the electric field). Finally, from Eqs. (30) and (31), and $f=\rho_{e0}$ when $\zeta\to 0$, we have

$$\psi_1(0)=s, \quad \rho_{e1}(0)=\frac{sf'}{s+f}. \tag{39}$$

We collect the results (35), (38), and (39) to obtain in the limit of $\zeta\uparrow 0$

$$\begin{pmatrix}\rho_{e1}\\ \rho_{i1}\\ \psi_1\\ \phi_1\end{pmatrix}\xrightarrow{z\uparrow 0}\begin{pmatrix}sf'(v)/(1+s/f(v))\\ 0\\ s\\ (vk-s)/k\end{pmatrix}. \tag{40}$$

The other boundary conditions at $\zeta=-\infty$ are that the total charge equals zero and the electric field vanishes. These conditions can be expressed as

$$\begin{pmatrix}\rho_{e1}\\ \rho_{i1}\\ \psi_1\\ \phi_1\end{pmatrix}\xrightarrow{\zeta\downarrow -\infty}\begin{pmatrix}\rho_{e1}^-\\ \rho_{e1}^-\\ 0\\ \phi_1^-\end{pmatrix}, \tag{41}$$

where ρ_{e1}^- and ϕ_1^- are constants.

VII. DISPERSION CURVE

In Sec. VI we formulated an eigenvalue problem. Given k, we want to find $s(k)$ such that there is a solution for the transverse perturbation equations (28) fulfilling the boundary conditions, Eqs. (40) and (41). In general, an analytic treatment for any value of k is not possible, and we have to resort to numerical calculations.[23] However, in the limits of small and large wave number, the equations simplify, and we can obtain the asymptotic behavior of the dispersion relation $s(k)$.

We start with the small k-limit. If Eqs. (28) and (29) are evaluated only to first order in k, ϕ_1 decouples and we obtain

$$\partial_\zeta\begin{pmatrix}\rho_{e1}\\ \rho_{i1}\\ \psi_1\end{pmatrix}=\mathbf{N}_{s,k}\cdot\begin{pmatrix}\rho_{e1}\\ \rho_{i1}\\ \psi_1\end{pmatrix}-\begin{pmatrix}\partial_\zeta\rho_e/(v+E)\\ \partial_\zeta\rho_i/v\\ 0\end{pmatrix}+O(k^2), \tag{42}$$

where

$$\mathbf{N}_{s,k}=\begin{pmatrix}\dfrac{s+2\rho_e-f-\rho_i}{v+E} & \dfrac{-\rho_e}{v+E} & \dfrac{\partial_\zeta\rho_e-\rho_e f'}{v+E}\\ \dfrac{-f}{v} & \dfrac{s}{v} & \dfrac{-\rho_e f'}{v}\\ 1 & -1 & 0\end{pmatrix}+O(k^2) \tag{43}$$

is the truncated matrix $\mathbf{M}_{s,k}$ (29). The fourth decoupled equation is

$$\partial_\zeta\phi_1=\psi_1. \tag{44}$$

The boundary condition (40) is

$$\begin{pmatrix}\rho_{e1}\\ \rho_{i1}\\ \psi_1\end{pmatrix}\xrightarrow{\zeta\uparrow 0}\begin{pmatrix}f'/(1+s/f)\\ 0\\ 1\end{pmatrix}+O(k^2), \tag{45}$$

and

$$\phi_1(0)=\frac{vk-s}{sk}=\frac{v}{s}-\frac{1}{k}. \tag{46}$$

Equations (44) and (46) give a condition on ψ_1:

$$\frac{vk-s}{sk}=\int_{-\infty}^{0}\psi_1(\zeta)d\zeta. \tag{47}$$

Consider now the limit $s\ll f(v)$. Then Eqs. (42) and (45) become identical up to order $s/f(v)$ to the perturbed equations obtained from an infinitesimal change of E_∞. If we compare two uniformly translating fronts with infinitesimally different field E_∞ at identical positions, their linearized difference solves the same equations. In this case, ψ_1 is independent of s and k. But then Eq. (47) implies that

$$s=vk+O(k^2) \quad \text{for } k\ll\alpha(v). \tag{48}$$

Equation (48) has an immediate physical interpretation: $1/k$ is the largest length scale involved. It is much larger than the thickness of the screening charge layer. Therefore the charge layer can be contracted to a δ-function contribution along an interface line. Such a screening charged interface has an instability at $s=vk$.

In the opposite limit of k sufficiently large, we also can find a relation for the dispersion. We make the assumption that the ion and electron densities remain bounded and use Eq. (28) to write the equations for ψ_1 and ϕ_1 as

$$\partial_\zeta\psi_1\simeq k^2(\phi_1+E), \tag{49a}$$

$$\partial_\zeta\phi_1=\psi_1. \tag{49b}$$

On the short length scale, $1/k$, the unperturbed electric field for $\zeta<0$ can be approximated by making an asymptotic expansion of Eqs. (23)–(25):[23]

$$E\simeq -v-f(v)\zeta, \tag{50}$$

If we substitute Eq. (50) into Eq. (49a), we obtain

$$\partial_\zeta^2\phi_1=k^2(\phi_1-v-f(v)\zeta). \tag{51}$$

The boundary condition (40) fixes $\phi_1(0)=(vk-s)/k$ and $\psi_1(0)=\partial_\zeta\phi_1=s$. The unique solution of Eq. (51) with these initial conditions is

$$\phi_1(\zeta)=v+f(v)\zeta-\frac{f(v)}{2k}e^{k\zeta}+\frac{f(v)-2s}{2k}e^{-k\zeta} \tag{52}$$

for $\zeta<0$. The mode $e^{-k\zeta}$ would increase rapidly toward decreasing ζ, create diverging electric fields in the ionized region, and cannot be balanced by any other terms in the equation. Therefore it has to be absent. The requirement that its coefficient $(f(v)-2s)/2k$ vanishes fixes the dispersion relation

$$s(k)=\frac{f(v)}{2}+O(k^{-1}) \quad \text{for } k\gg\alpha(v). \tag{53}$$

Again there is a simple physical interpretation of this growth rate. The electric field can be approximated in leading order by

$$\mathbf{E}(x,\zeta,t)\simeq\begin{cases}-(v+f(v)\zeta) & (\zeta<0)\mathbf{e}_z,\\ -v\,\mathbf{e}_z & (\zeta>0).\end{cases} \tag{54}$$

When the discontinuity propagates with the local field $v=-E$, a perturbation in the field $\mathbf{E}=-\hat{z}(v+\partial_\zeta E\zeta)$ will grow with the rate $\partial_\zeta E$. The averaged slope of the field for $\zeta>0$ and $\zeta<0$ is $\partial_\zeta E=f(v)/2$, and this slope is precisely the growth rate in Eq. (53) determined previously.

We have studied the (in)stability of planar negative ionization fronts against linear perturbations and have found

$$s(k)=\begin{cases}|E_\infty|k & (k\ll\alpha(|E_\infty|)),\\ |E_\infty|\alpha(|E_\infty|)/2 & (k\gg\alpha(|E_\infty|)).\end{cases} \tag{55}$$

Thus, the planar front becomes unstable with a linear growth rate $s(k)$ for small k to a saturation value $|E_\infty|\alpha(|E_\infty|)/2$. This instability gives us a mechanism for branching. For the case of a curved front, if the radius of curvature increases, the planar approximation for the tip is reasonable and allows a qualitative understanding of the branching phenomena.

VIII. SUMMARY AND OUTLOOK

In this paper a fully deterministic model for streamers is suitable for noninteracting gases such as nitrogen without photoionization was presented. We have proposed that an anode directed front can branch spontaneously according to this model due to Laplacian interfacial instability. We showed some numerical evidence of this phenomena. We have studied the stability of a planar front and how a transverse perturbation would grow. The dispersion curve for the planar case gives us a qualitative picture of the mechanism acting on a curved front. We also have calculated the asymptotic behavior of the dispersion curve.

However, some questions remain. From the dispersion curve an instability will grow for a sufficiently short wavelength. We expect that a regularization mechanism should come into play. The regularization mechanism that selects a particular mode could be the electric screening due to curvature.[23] Another possibility is diffusion phenomena, which we did not consider in the shock front case. Diffusion was neglected to prevent mathematical challenges, but sooner or later we have to face this challenge.

The physics of low temperature plasmas is an area where many fundamental questions still remain unanswered, and where experiments have been ahead of theory. When I hear some pessimistic voices for the future of physics, I think there is much room at the bottom to enjoy the show.

[a]Electronic mail: m.arrayas@escet.urjc.es

[1]"Saint Elmo's Fire." Encyclopaedia Britannica, ⟨http://www.britannica.com⟩.
[2]For a tutorial on display technologies, see ⟨http://www.atip.org/fpd/src/tutorial/fpd.html⟩.
[3]*Electrical Discharges for Environmental Purposes: Fundamentals and Applications*, edited by E. M. van Veldhuizen (NOVA Science, New York, 1999).
[4]Y. P. Raizer, *Gas Discharge Physics* (Springer, Berlin, 1991).
[5]V. P. Pasko, M. A. Stanley, J. D. Mathews, U. S. Inan, and T. G. Wood, "Electrical discharge from a thundercloud top to the lower ionosphere," Nature (London) **416**, 152–154 (2002).
[6]There is a wonderful web site with pictures of sprites, blue jets, and lightning: ⟨http://www.sky-fire.tv⟩.
[7]H. Raether, "Die Entwicklung der Elektronenlawine in den Funkenkanal," Z. Phys. **112**, 464–489 (1939).
[8]L. Niemeyer, L. Pietronero, and H. J. Wiesmann, "Fractal dimension of dielectric breakdown," Phys. Rev. Lett. **52**, 1033–1036 (1984).
[9]M. Arrayás, U. Ebert, and W. Hundsdorfer, "Spontaneous branching of anode-directed streamers between planar electrodes," Phys. Rev. Lett. **88**, 174502-1–174502-4 (2002).
[10]W. van Saarloos, "Three basic issues concerning interface dynamics in nonequilibrium pattern formation," Phys. Rep. **301**, 9–43 (1998).
[11]When an electron collides with a neutral gas atom or molecule, it may become attached, forming a negative ion. This process depends on the energy of the electron and the nature of the gas.
[12]U. Ebert, W. van Saarloos, and C. Caroli, "Streamer propagation as a pattern formation problem: Planar fronts," Phys. Rev. Lett. **77**, 4178–4181 (1996) and "Propagation and structure of planar streamer fronts," Phys. Rev. E **55**, 1530–1549 (1997).
[13]S. K. Dhali and A. P. Pal, "Numerical simulation of streamers in SF_6," J. Appl. Phys. **63**, 1355–1362 (1988).
[14]F. A. Williams, *Combustion Theory* (Benjamin/Cummings, Menlo Park, 1985).
[15]P. Pelcé, *Dynamics of Curved Fronts* (Academic, Boston, 1988).
[16]P. A. Vitello, B. M. Penetrante, and J. N. Bardsley, "Simulation of negative-streamer dynamics in nitrogen," Phys. Rev. E **49**, 5574–5598 (1994).
[17]P. Wesseling, *Principles of Computational Fluid Dynamics*, Springer Series in Computational Mathematics (Springer, Berlin, 2001).
[18]A. Rocco, U. Ebert, and W. Hundsdorfer, "Branching of negative streamers in free flight," Phys. Rev. E **66**, 035120-1–035120-4 (2002).
[19]See reply letter by U. Ebert and W. Hundsdorfer, Phys. Rev. Lett. **89**, 229402 (2002) on the comment by A. A. Kulikovsky, *ibid.* **89**, 229401 (2002).
[20]A. N. Lagarkov and I. M. Rutkevich, *Ionization Waves in Electrical Breakdown in Gases* (Springer, New York, 1994).
[21]U. Ebert and W. van Saarloos, "Front propagation into unstable states: Universal algebraic convergence towards uniformly translating pulled fronts," Physica D **146**, 1–99 (2000).
[22]The book is freely available at ⟨http://www.nr.com⟩.
[23]M. Arrayás and U. Ebert, "Stability of negative ionization fronts: Regularization by electric screening?," Phys. Rev. E **69**, 036214-1–036214-8 (2002).